Epigenetic signature of PD-1+ TCF1+ CD8 T cells that act as resource cells during chronic viral infection and respond to PD-1 blockade

Rohit R. Jadhav[a,b,1], Se Jin Im[c,1], Bin Hu[a,b,1], Masao Hashimoto[c], Peng Li[d], Jian-Xin Lin[d], Warren J. Leonard[d], William J. Greenleaf[e,f,g], Rafi Ahmed[c,2], and Jorg J. Goronzy[a,b,2]

[a]Division of Immunology and Rheumatology, Department of Medicine, Stanford University, Stanford, CA 94305; [b]Department of Medicine, Palo Alto Veterans Administration Healthcare System, Palo Alto, CA 94306; [c]Emory Vaccine Center, Emory University School of Medicine, Atlanta, GA 30322; [d]Laboratory of Molecular Immunology, Immunology Center, National Heart, Lung, and Blood Institute, National Institutes of Health, Bethesda, MD 20892; [e]Center for Personal Dynamic Regulomes, Stanford University, Stanford, CA 94305; [f]Department of Genetics, Stanford University, Stanford, CA 94305; and [g]Department of Applied Physics, Stanford University, Stanford, CA 94305

Contributed by Rafi Ahmed, May 17, 2019 (sent for review March 1, 2019; reviewed by Nina Bhardwaj and Stephen C. Jameson)

We have recently defined a novel population of PD-1 (programmed cell death 1)+ TCF1 (T cell factor 1)+ virus-specific CD8 T cells that function as resource cells during chronic LCMV infection and provide the proliferative burst seen after PD-1 blockade. Such CD8 T cells have been found in other chronic infections and also in cancer in mice and humans. These CD8 T cells exhibit stem-like properties undergoing self-renewal and also differentiating into the terminally exhausted CD8 T cells. Here we compared the epigenetic signature of stem-like CD8 T cells with exhausted CD8 T cells. ATAC-seq analysis showed that stem-like CD8 T cells had a unique signature implicating activity of HMG (TCF) and RHD (NF-κB) transcription factor family members in contrast to higher accessibility to ETS and RUNX motifs in exhausted CD8 T cells. In addition, regulatory regions of the transcription factors *Tcf7* and *Id3* were more accessible in stem-like cells whereas *Prdm1* and *Id2* were more accessible in exhausted CD8 T cells. We also compared the epigenetic signatures of the 2 CD8 T cell subsets from chronically infected mice with effector and memory CD8 T cells generated after an acute LCMV infection. Both CD8 T cell subsets generated during chronic infection were strikingly different from CD8 T cell subsets from acute infection. Interestingly, the stem-like CD8 T cell subset from chronic infection, despite sharing key functional properties with memory CD8 T cells, had a very distinct epigenetic program. These results show that the chronic stem-like CD8 T cell program represents a specific adaptation of the T cell response to persistent antigenic stimulation.

CD8 T cell exhaustion | ATAC-seq | epigenetic profiles

In contrast to the highly functional memory CD8 T cells that are generated following resolution of an acute viral infection, continuous antigenic stimulation results in various stages of T cell dysfunction (1). This functional exhaustion of CD8 T cells has been documented during chronic viral infections as well as cancer (2–8). A characteristic feature of exhausted CD8 T cells is expression of various inhibitory receptors, most notably PD-1 (programmed cell death 1) (9, 10). PD-1 is the dominant inhibitory receptor regulating CD8 T cell exhaustion, and blockade of this inhibitory pathway restores T cell function in vivo (6, 9, 11, 12). This provided the cellular basis for the development of PD-1–directed immunotherapy that is now licensed for use in several different cancers (13).

Recent studies have provided more clarity and insight on the nature of T cell exhaustion during chronic viral infection. We recently identified a novel population of PD-1+ TCF1 (T cell factor 1)+ virus-specific CD8 T cells that function as resource cells during chronic LCMV infection of mice (14). These CD8 T cells are quiescent, do not express effector molecules, and are found in lymphoid tissues where they reside predominantly in T cell zones (14). These CD8 T cells display stem cell-like properties and undergo a slow self-renewal, and also differentiate to give rise to the more terminally differentiated/exhausted CD8 T cells that are found at the major sites of infection in both lymphoid and nonlymphoid tissues. The transcription factor TCF1 is essential for the generation of this stem-like CD8 T cell population during chronic infection. Importantly, the proliferative burst of T cells observed after PD-1 blockade comes exclusively from these PD-1+ TCF1+ stem-like CD8 T cells (14). Thus, these cells are critical for the effectiveness of PD-1 therapy. Several other studies have confirmed and extended our observations showing that such stem-like CD8 T cells are generated in other chronic viral infections in mice and also in nonhuman primate and human chronic infections (15–21). In addition, there has been a series of papers during the past year documenting the presence of these PD-1+ TCF1+ CD8 T cells in human cancer and also data

Significance

PD-1+ TCF1+ stem-like CD8 T cells are critical for maintaining the T cell response during chronic viral infection and cancer, and provide the proliferative burst seen after PD-1 immunotherapy. These cells undergo a slow self-renewal and also give rise to the more terminally differentiated and exhausted CD8 T cells. Here we define the epigenetic landscape of the stem-like CD8 T cells and their more differentiated progeny. These 2 CD8 T cell subsets from chronically infected mice showed substantial differences, but also shared common features that were distinct from the epigenetic signature of effector and memory CD8 T cells generated after an acute viral infection. This information will be useful in targeting epigenetic changes to improve current immunotherapies.

Author contributions: S.J.I., B.H., W.J.G., R.A., and J.J.G. designed research; R.R.J., S.J.I., B.H., M.H., P.L., and J.-X.L. performed research; R.R.J. and S.J.I. analyzed data; and R.R.J., S.J.I., B.H., W.J.L., R.A., and J.J.G. wrote the paper.

Reviewers: N.B., Icahn School of Medicine at Mount Sinai; and S.C.J., University of Minnesota.

The authors declare no conflict of interest.

This open access article is distributed under Creative Commons Attribution-NonCommercial-NoDerivatives License 4.0 (CC BY-NC-ND).

Data deposition: The ATAC-seq data have been deposited in in the National Center for Biotechnology Information BioProject database (https://www.ncbi.nlm.nih.gov/bioproject/) under accession no. PRJNA546023. The RNA-seq data have been deposited in the Gene Expression Omnibus database (https://www.ncbi.nlm.nih.gov/geo) under accession no. GSE132110.

[1]R.R.J., S.J.I., and B.H. contributed equally to this work.

[2]To whom correspondence may be addressed. Email: rahmed@emory.edu or jgoronzy@stanford.edu.

This article contains supporting information online at www.pnas.org/lookup/suppl/doi:10.1073/pnas.1903520116/-/DCSupplemental.

Published online June 21, 2019.

Downloaded at Stanford University on November 16, 2021

suggesting that the frequency of these cells was associated with the clinical outcome of checkpoint immunotherapy (22–24).

Epigenetics plays an important role in regulating the development, differentiation, and function of T cells (25). In this study, we have done ATAC-seq (assay for transposase-accessible chromatin using sequencing) analysis of these newly defined stem-like CD8 T cells from LCMV chronically infected mice and compared it with the epigenetic profile of the more terminally differentiated (exhausted) CD8 T cells. In addition, we have compared the epigenetic signature of the stem-like cells generated during chronic infection with effector and memory CD8 T cells generated following an acute LCMV infection. The epigenetic signature of the stem-like CD8 T cells from chronically infected mice was different not only from the exhausted CD8 T cells but also distinct from the epigenetic profile of effector and memory CD8 T cells generated during acute infection.

Results and Discussion

Chromatin Accessibility Landscapes in Stem-Like and Exhausted CD8 T Cells During Chronic Viral Infection. To determine how the stem-like and exhausted CD8 T cell subsets differ from each other at the epigenetic level and which transcription factor networks account for their distinct differentiation states, we sorted PD-1+ CXCR5+ Tim-3− stem-like and PD-1+ CXCR5− Tim-3+ exhausted CD8+ T cells from the spleens of mice chronically infected with LCMV on day 45 postinfection (*SI Appendix*, Fig. S1*A*). We generated genome-wide maps of chromatin accessibility using ATAC-seq (26). Principal component analysis (PCA) of the 5,000 most variably accessible sites segregated stem-like and exhausted CD8 T cells into 2 clearly separate clusters distinct from naïve CD8 T cells (Fig. 1*A*). To determine the epigenomic markers defining the subset identity of these 2 functionally distinct subsets of T cells, we identified sites of differential accessibility using DESeq2 (27) (Fig. 1*B*). Using 1.5-fold log2 difference and $P < 0.001$ as cutoff, we found a similar number of sites differentially open ($n = 3{,}584$) or closed ($n = 3{,}450$) in the stem-like T cells compared with the exhausted T cells. Sequencing read densities at genes encoding the subset-defining phenotypic markers are shown in *SI Appendix*, Fig. S1*B*. Both subsets displayed the same chromatin accessibility pattern at or adjacent to the *Pdcd1* (encoding PD-1) locus, and accessibility at the transcription start sites (TSSs) of *Cxcr5* and *Havcr2* (encoding Tim-3) reflected the cell-surface marker profile used for purification of these 2 subsets.

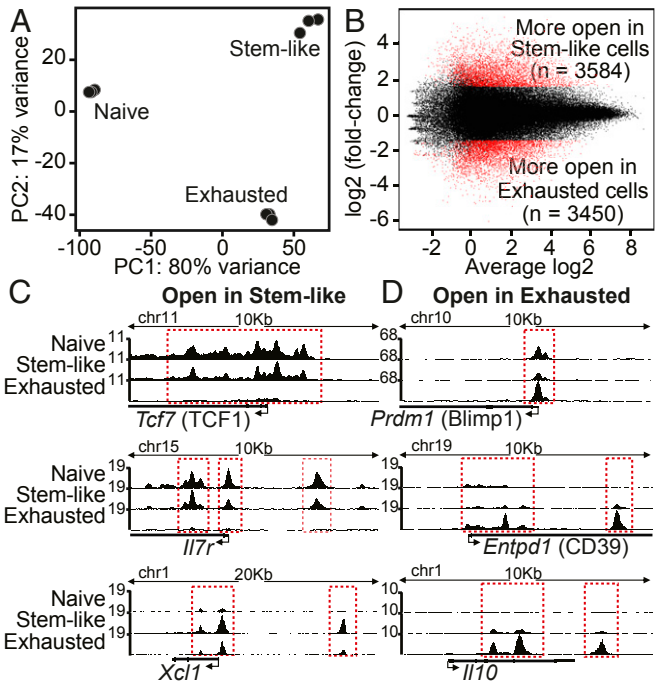

Fig. 1. Chromatin accessibility profiles of antigen-specific CD8 T cell subsets in chronic LCMV infection. PD-1+ CXCR5+ Tim-3− stem-like and PD-1+ CXCR5− Tim-3+ exhausted CD8 T cells were isolated from LCMV chronically infected mice on day 45 after infection. Naïve ($CD44^{lo}$) CD8 T cells were sorted from uninfected mice. Chromatin accessibility profiles of sorted CD8 T cell subsets were examined using ATAC-seq analysis. (*A*) PCA based on the 5,000 most variable peaks. (*B*) Scatter plot (MA plot) of log-2-fold (log2 FC) differences between stem-like and exhausted T cells versus the mean of normalized logCPM (count-per-million). Red indicates sites that were significantly different (adjusted *P* value < 0.001, log2 FC > 1.5). (*C* and *D*) Accessibility tracks for selected genes significantly more open in stem-like CD8 T cells (*C*) or exhausted CD8 T cells (*D*) in chronic LCMV infection.

Sequencing read densities at a few selected genes of subset-specific functional importance are shown in Fig. 1 *C* and *D* and *SI Appendix*, Fig. S1 *C* and *D* Stem-like CD8 T cells contained open peaks for *Tcf7* (TCF1), *Il7r*, *Xcl1*, *Bcl6*, *Ccr7*, and *Cd28* (Fig. 1*C* and *SI Appendix*, Fig. S1*C*). The *Cd28* peak is about half open. This pattern is consistent with their known biological properties (14). TCF1 is essential for the generation of the stem-like CD8 T cells, CCR7 is important for localization in the T cell zones, and CD28 signaling is required for the proliferation of stem-like CD8 T cells after PD-1 blockade (14, 28). In particular, the *Xcl1* locus is highly open in stem-like cells compared with exhausted cells. XCL1 attracts type 1 conventional dendritic cells (cDC1s) including CD8α+ lymphoid DCs, which exclusively express XCR1. Our recent discovery of a stem-like CD8 T cell subset, in combination with our observation that B7–CD28 interaction is necessary for the proliferative burst seen after PD-1 blockade (14, 28), is of interest to examine the role of DCs, especially cDC1s, in the proliferation of virus-specific CD8 T cells after PD-1–directed immunotherapy. Exhausted CD8 T cells exhibited a different pattern with open peaks for *Prdm1* (Blimp1, half open) that is involved in differentiation into terminal effector CD8 T cells (29) and *Heyl* that promotes the differentiation of neuronal progenitor cells (30) (Fig. 1*D* and *SI Appendix*, Fig. S1*D*). In addition, the inhibitory receptors [*Cd244* (2B4) and *Entpd1* (CD39)] and the regulatory cytokine *Il10* were exclusively open in exhausted CD8 T cells. Consistent with their more differentiated state, these cells were open in effector molecules such as *Gzmb*. Taken together, these results document distinct epigenetic profiles between stem-like and exhausted CD8 T cells during chronic LCMV infection.

Gene Networks Controlled by Proximal Regulatory Regions Distinguishing Stem-Like and Exhausted CD8 T Cells. We identified 766 genes within 10 kb of 941 peaks that were significantly more open in stem-like cells and 851 genes within 10 kb of 1,016 sites that were significantly more open in exhausted cells. Ingenuity pathway analysis of differentially accessible genes was used to generate networks that included a maximum of 35 genes and had a score of more than 1 (*SI Appendix*, Table S1). For both subsets, there was one network where all 35 included genes were near sites of increased accessibility. The network structures are shown in *SI Appendix*, Fig. S2*A* for stem-like T cells and *SI Appendix*, Fig. S2*B* for exhausted T cells, overlaid by gene expression values from RNA-seq analysis. Overall, we see a correlation between chromatin accessibility and gene transcription. Twenty-nine of the 35 more accessible genes were also overexpressed at the transcript levels in stem-like cells (indicated by red color, *SI Appendix*, Fig. S2*A*). The network is centered on *Il2* and *Id3*, which are more accessible as well as more transcribed in stem-like cells. In agreement with a previously reported study in LCMV and tumors (24), we also found that stem-like CD8 T cells had increased accessibility and transcription of *Slamf6* (encoding Ly108). It includes a set of transcriptional regulator

Downloaded at Stanford University on November 16, 2021

genes that have been shown to be involved in memory cell development, including *Tcf7*, *Id3*, and *Bach2* (29). This resemblance indicates that this transcription factor (TF) network maintains the functionality and survival of stem-like CD8 T cells in chronically infected mice. Moreover, we see increased accessibility and transcription in stem-like cells for *Satb1*, which has been suggested to regulate PD-1 expression (31).

The network with the best fit for genes more accessible in exhausted cells is shown in *SI Appendix*, Fig. S2*B*. Thirty-one of the 35 more accessible genes are also more transcribed in exhausted cells. Many of these genes are related to cytotoxic effector function, including *Gzmb* and markers of NK cells such as *Cd244* (2B4) and *Klrb1*, and to migration such as chemokines and chemokine receptors. *Il10* has a central position in this network and is more accessible as well as more transcribed in exhausted cells. TFs included in this network are *Prdm1*, *Runx2*, *Irf4*, and *Stat5a*, which are known to be involved in effector differentiation (29, 32–34).

Functional Annotation of Differentially Accessible Distal Regulatory Regions in Stem-Like and Exhausted CD8 T Cells. To include distal *cis*-regulatory regions of functional genes, we applied the Genomic Regions Enrichment of Annotations Tool (GREAT). The majority of differentially accessible regions were mapped to *cis*-regulatory regions between 5 and 50 or 50 and 500 kb from the TSS (*SI Appendix*, Fig. S3*A*). Multiples of these genes had several peaks assigned, ranging up to 25 peaks (*SI Appendix*, Fig. S3*B*). We identified 2,520 genes with more accessible regulatory regions in stem-like cells, 35 of which had ≥10 differentially open sites. As shown in *SI Appendix*, Fig. S3*C*, genes with multiple differentially open sites tended to also be more expressed. Functional annotation clustering of genes with ≥5 sites showed enrichment for genes involved in cytokine–cytokine receptor interaction and in WNT signaling as dominant pathways. Conversely, GREAT identified 2,946 genes with more accessible regulatory regions in exhausted cells, 16 of them with ≥10 more open sites. The TFs *Id2* and *Prdm1* were the transcriptional regulators with the most differentially accessible regulatory domains (*SI Appendix*, Fig. S3*C*). Genes with multiple differentially open sites in exhausted cells were enriched for the GO term "signaling" in general and more specifically "TCR signaling" and "GTPase binding."

Fig. 2 summarizes the differentially accessible regions for immunologically relevant genes that have been implicated in influencing or determining the functional characteristics of stem-like and exhausted CD8 T cells in chronic infections. Accessibility patterns for selected TFs and chemokine receptors are clearly distinct and nearly mutually exclusive. Exhausted T cells are broadly epigenetically poised to express effector molecules, cytokines/chemokines, and negative regulators, while stem-like cells have increased accessibility to memory genes, chemokines like *Xcl1*, and cytokines such as *Il2*.

Transcription Factor Networks Controlling Stem-Like and Exhausted CD8 T Cells Inferred from Differentially Accessible Motifs. The results described so far have identified epigenetic differences that could account for differential expression of various TFs in the stem-like and exhausted CD8 T cells during chronic infection. To further associate these TF networks with the differentiation state of the 2 subsets, we calculated the enrichment of TF-binding motifs at sites that significantly differed in accessibility, using HOMER motif analysis software. At peaks more open in the stem-like cells, we found motifs for several members of the HMG, RHD, and TBX families as most significantly enriched (Fig. 3*A*, *Right*). Top hits encompassed *Tcf3*, *Tcf4*, and *Tcfl2* of the HMG family. *Tcf7*, the member most widely studied in T cells, is not included in the HOMER software, but has a similar binding motif as the other HMG members and is therefore equally enriched. Conversely, ETS and Runx motifs were enriched at sites more open in exhausted cells (Fig. 3*A*, *Left*). In addition, increased accessibility

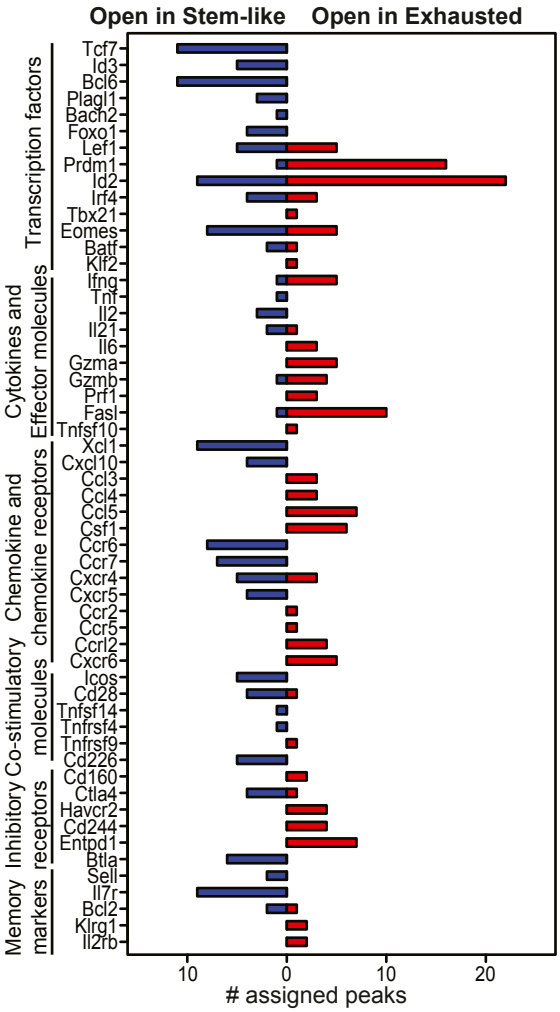

Fig. 2. Gene annotations of differentially accessible distal regulatory regions in stem-like and exhausted cells. The number of differentially open gene regulatory regions for genes of functional importance in stem-like (*Left*) and exhausted cells (*Right*).

was seen for a single member of the NR family, *Nur77*, which is an early response gene indicative of TCR-mediated activation (35).

As an alternative approach to infer TF networks, we used chromVAR, an analytical tool recently developed to identify motifs associated with variability in chromatin accessibilities between individual cells or samples. Results from triplicate experiments of naïve CD8 T cells and the CD8 T cell subsets from chronically infected mice are shown in *SI Appendix*, Fig. S4. Compared with naïve T cells, both subsets shared increased openness at bZIP, T-box, and NUR77 motifs. Sites displaying motifs for members of the bZIP family including *Batf* were equally open in stem-like and exhausted cells. A few members of the bZIP family, such as *Atf2* and *Atf7*, were more accessible in exhausted T cells, but differences were small. Striking differences between the 2 subsets were seen for TCF and NF-κB motifs, which were accessible in the stem-like but not in the exhausted T cells. Conversely, ETS motifs were not accessible in stem-like cells, setting them apart not only from exhausted but also naïve CD8 T cells. Increased accessibility to ETS motifs in naïve and exhausted CD8 T cells involved different peak sets that only overlapped by less than 5%. To determine whether these 2 different peak sets are enriched for motifs of distinct TFs, we identified ETS motif-containing peaks that were differentially

Downloaded at Stanford University on November 16, 2021

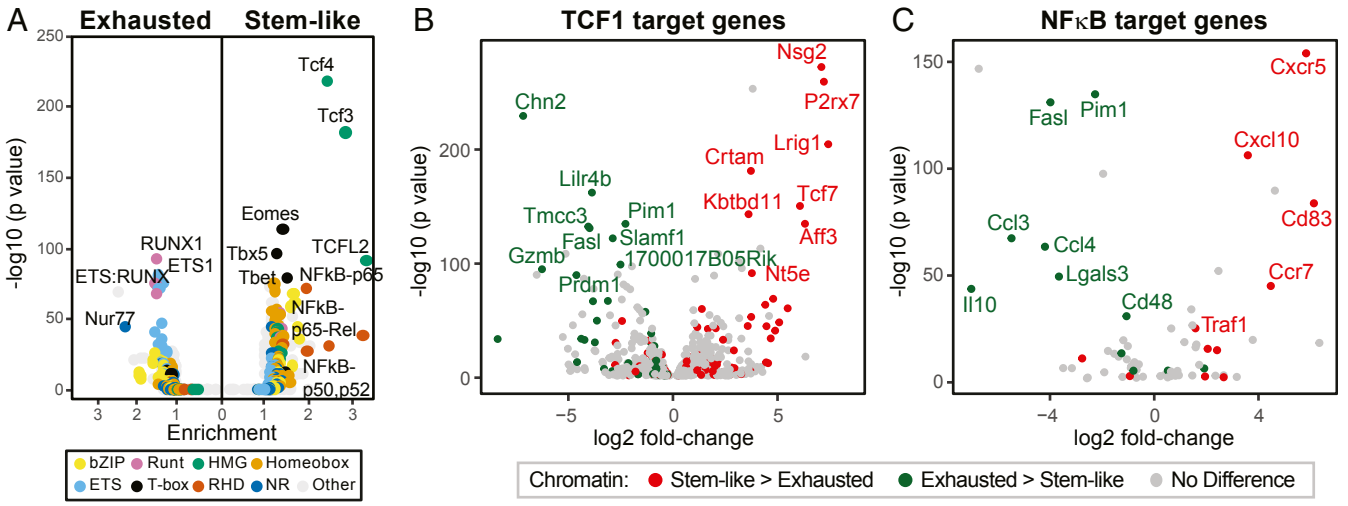

Fig. 3. Chromatin accessibility peaks are associated with distinct transcription factor families in stem-like and exhausted cells. (*A*) TF family binding motifs enriched in loci more accessible in stem-like (*Right*) or exhausted cells (*Left*); the *x* axis shows the enrichment factor (ratio of the percentage of differential sites with motifs to the percentage of nondifferential sites with motifs), and the *y* axis shows the significance level of enrichment. TF families are indicated by color code. (*B* and *C*) Volcano plots of expression levels of TCF1 (*B*) and NF-κB target genes (*C*) in stem-like vs. exhausted T cells. The color code identifies target genes that were close to a differentially accessible site, with red indicating increased and green indicating reduced openness in stem-like cells.

accessible in naïve and exhausted CD8 T cells. We found TCF motifs enriched in the peaks more accessible in naïve T cells and bZIP motifs enriched at sites more accessible in exhausted cells, consistent with their naïve and effector state.

Binding-motif analysis of accessible chromatin sites implicated different TF networks in stem-like and exhausted T cells. To confirm the functional relevance of these TF networks, we compared the transcriptome of these 2 T cell subsets for expression of the respective TF target genes. The epigenome of stem-like cells was most strikingly characterized by increased openness to 2 binding motifs, one common to several TCF members of the HMG family and one motif shared by NF-κB members of the RHD family. In our transcriptome analysis, we focused on TCF1 (encoded by *Tcf7*) that we previously found to be obligatory for generating stem-like T cells (14). Of 1,438 target genes, we found 359 significantly down-regulated and 379 up-regulated (Fig. 3*B*). Thus, more than 50% of TCF target genes were differentially expressed in the 2 subpopulations, reflecting highly significant enrichment for TCF1 target genes among differentially expressed genes (P = 3.56e-21). As illustrated by the color code in the volcano plot in Fig. 3*B*, differential accessibility as determined by ATAC-seq highly correlated with differential expression of target genes. Expression of NF-κB target genes, taken as representative for the RHD family motif more accessible in stem-like cells, significantly differed in stem-like and exhausted cells (P = 3e-6), again closely aligned with differential chromatin accessibility (Fig. 3*C*). NF-κB–regulated genes included several molecules involved in trafficking such as *Cxcr5*, *Ccr7*, and *Cxcl10*, which were more accessible in stem-like cells.

Distinct Epigenetic Differentiation Trajectories of CD8 T Cells During Chronic versus Acute Viral Infection. We next compared the epigenetic signatures of the 2 chronic CD8 T cell subsets with effector and memory CD8 T cells generated following an acute infection. Of particular interest was the question of whether the stem-like CD8 T cells that embody many functional characteristics of memory CD8 T cells, such as ability to proliferate and differentiate and also undergo self-renewal, would have an epigenetic signature that was similar to memory CD8 T cells or have a signature distinct from memory CD8 T cells generated after an acute infection.

To address this question, we isolated virus-specific effector CD8 T cells from the spleen at day 8 after an acute LCMV infection and memory CD8 T cells at 45 d after infection. In this acute LCMV Armstrong infection mouse model, the virus is cleared within 1 wk by a vigorous LCMV-specific CD8 T cell response (36). The day 8 LCMV-specific effector CD8 T cells were further subdivided into terminal effector ($CD127^{lo}KLRG1^{hi}$) and memory precursor ($CD127^{hi}KLRG1^{lo}$) cells. These cells will be referred to as d8 TE and d8 MP. Previous studies have shown that most of the day 8 TE cells die whereas the day 8 MP cells survive and give rise to the pool of long-lived memory CD8 T cells (37–40). We did ATAC-seq analysis of these 5 different populations plus naïve CD8 T cells and, to obtain a global assessment of the epigenetic relationships of the different subsets, we performed PCA on the 5,000 most variable sites (Fig. 4*A*). The 2 subsets obtained from chronically infected mice formed 2 clearly separate clusters, but quite strikingly both the chronic T cell subsets were distant from the cluster formed by the CD8 T cells (d8 TE, d8 MP, and memory) from acute infection. To determine whether there are common features shared by both subsets from chronically infected mice that set them apart from memory cells from acutely infected mice, we compared the sites that were differentially accessible. Sites identified in exhausted and stem-like cells were frequently shared, both for sites significantly more open as well as more closed in memory cells (*SI Appendix*, Fig. S5*A*), and fold differences in openness correlated (r^2 = 0.4; *SI Appendix*, Fig. S5*B*). For example, they both displayed the chromatin accessibility patterns adjacent to the *Pdcd1* locus with a peak unique for chronically infected mice (Fig. 4*B*). Moreover, both chronic subsets (stem-like and exhausted) shared increased accessibilities to *Tox* (Fig. 4*B*). This demonstrates a common programming for chronic infection and not necessarily for functional impairment.

Nevertheless, exhausted and stem-like T cells had clearly distinctive features that could be traced back to naïve or effector T cells. As illustrated in Fig. 4*C*, we compared how sites more accessible in exhausted or in stem-like CD8 T cells appear in naïve T cells or different subsets after acute infection. Results are shown as peak-centered heatmaps of ATAC-seq read densities. The accessibility pattern in stem-like cells was more similar to naïve T cells, while the pattern in exhausted T cells showed some overlap with that of terminal effector T cells on day 8 after acute infection.

This distinctiveness of each subset is also evident in the TF networks implicated through chromVAR analysis of all subsets from acutely and chronically infected mice (*SI Appendix*, Fig. S6*A*). The deviation scores were normalized across all TFs within

Downloaded at Stanford University on November 16, 2021

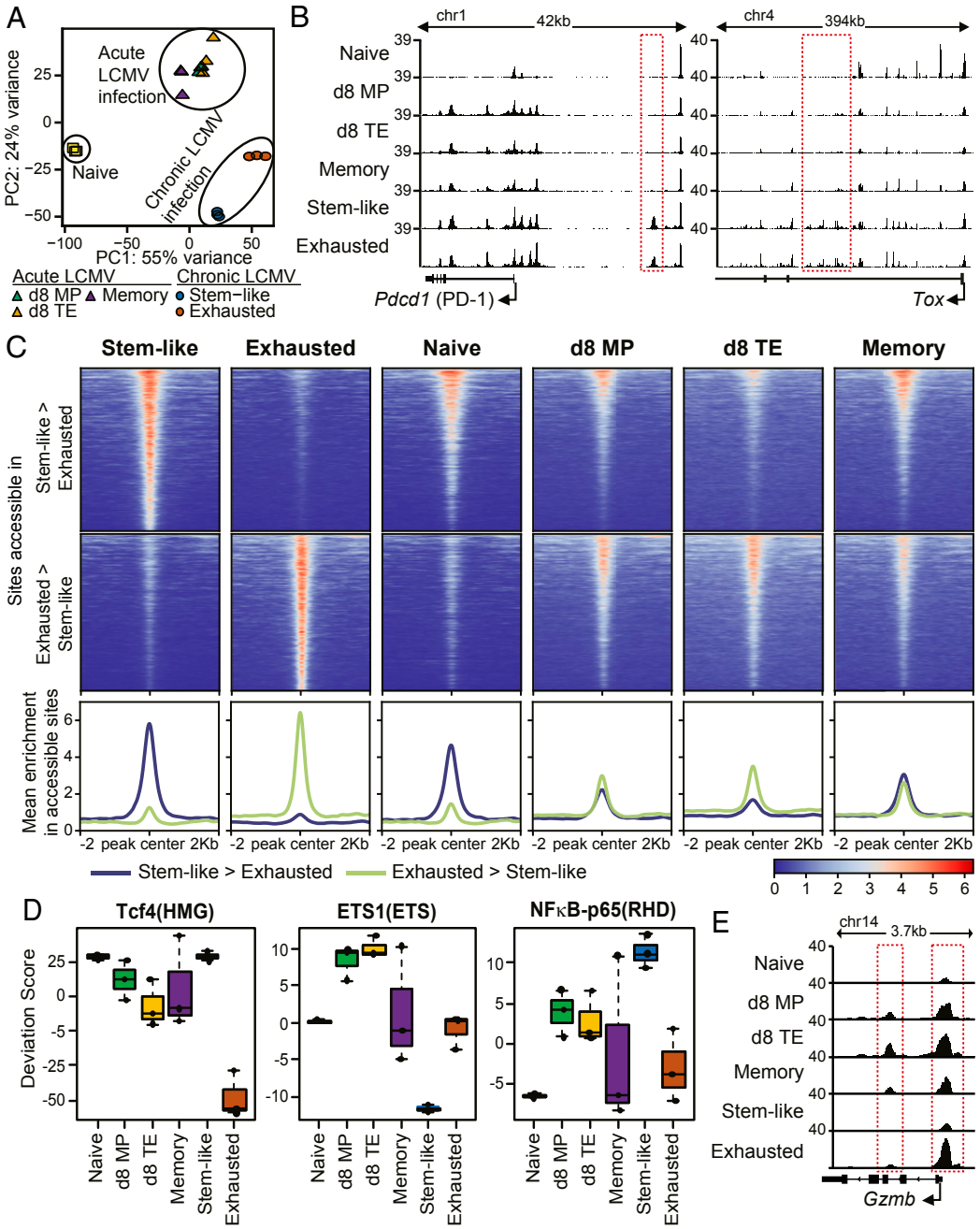

Fig. 4. Distinct chromatin signatures in stem-like and exhausted T cells from chronically infected mice compared with effector and memory T cells after acute infection. Stem-like and exhausted T cells from chronically infected mice (d45), naïve CD8 T cells from uninfected mice, and LCMV-specific memory precursor ($CD127^{hi}KLRG1^{lo}$, d8 MP), terminal effector ($CD127^{lo}KLRG1^{hi}$, d8 TE), and memory T cells (d45) from acutely infected mice are compared. (*A*) PCA based on the 5,000 most variable peaks across the indicated 6 CD8 subpopulations. (*B*) Accessibility tracks for genes which are exclusively open in stem-like and exhausted CD8 T cells generated in chronic LCMV infection and different from effector and memory CD8 T cells generated by acute LCMV infection. (*C*) The heatmaps show the accessibility across ±2-kb regions around those sites that were significantly more open in stem-like (*Top*) or exhausted T cells (*Middle*). Line graphs (*Bottom*) show the average intensity of sites more accessible in stem-like (blue line) or in exhausted cells (green line) for these 6 subsets. (*D*) TF-motif deviation scores from chromVAR analysis for selected TFs are shown as box plots of triplicate measurements. (*E*) Accessibility track for *Gzmb* which is selectively closed in naïve and stem-like CD8 T cells.

each replicate to allow visualization of similarities or dissimilarities of the rank order of accessibility associated with different motifs between samples. Memory precursors and effectors, both taken on day 8 after acute infection, closely coclustered. Memory T cells collected after day 45 clustered most closely to naïve cells. The 2 T cell subsets from chronically infected mice formed very well defined and completely distinct clusters. Absolute deviation scores (not normalized across each sample) for selected TFs displaying highest accessibility variability across samples are shown as box plots from triplicate experiments for naïve CD8 T cells and the 5 subsets of LCMV-specific cells (d8 MP, d8 TE, and memory cells after acute infection, and stem-like and exhausted cells in chronic infections) in Fig. 4*D*. Additional box plots of deviation scores are shown in *SI Appendix*, Fig. S6*B* for TFs that are known to be

Downloaded at Stanford University on November 16, 2021

involved in T cell activation. The hallmark feature for exhausted T cells was that they had lost accessibility to TCF motifs, even more so than effector T cells during acute infection. Stem-like T cells were unique in that they have gained accessibility to NF-κB-p65 motifs while closing sites harboring ETS motifs (Fig. 4*D*). NUR77 and BATF accessibility was consistent with the activation state of the cell populations. ATF2 was unusual as a bZIP family member in that its motif was more accessible in exhausted cells. Surprisingly, NFAT sites were most accessible in stem-like cells, and both populations from chronically infected mice had lost accessibility for RUNX.

A particularly interesting epigenetic difference is seen at the granzyme B locus (Fig. 4*E*). The granzyme B locus is open in effector CD8 T cells that express large amounts of granzyme B during acute infection, and this locus remains open in memory CD8 T cells even after the viral infection is cleared and there is minimal to no granzyme B expression. Thus, the memory CD8 T cells generated after an acute viral infection are poised to rapidly express granzyme B (40, 41). Quite strikingly, the granzyme B locus is closed in the stem-like CD8 T cells from chronically infected mice, showing that these cells have acquired an epigenetic program to regulate granzyme B expression. This further highlights the differences between the stem-like CD8 T cells from chronically infected mice and memory CD8 T cells generated after an acute infection.

Perhaps the most interesting finding from these studies is that the stem-like CD8 T cells generated during chronic infection have a unique epigenetic signature that is distinct from effector and memory CD8 T cells generated during acute infection. Even though the stem-like CD8 T cells from chronic infection have captured some key biological properties of conventional memory CD8 T cells generated after an acute infection or vaccination, they exhibit a distinct transcriptional and epigenetic program. This clearly shows that these TCF1+ PD-1+ stem-like CD8 T cells represent a specific adaptation of the CD8 T cell response to chronic antigenic stimulation.

Materials and Methods

A detailed description of materials and methods is provided in *SI Appendix, Materials and Methods*. Memory precursor (CD127^{hi}KLRG1^{lo}) and terminal effector (CD127^{lo}KLRG1^{hi}) P14 CD8 T cells were sorted from acutely infected mice on day 8 postinfection. Memory P14 CD8 T cells from immune mice and PD-1+ CXCR5+ Tim-3− stem-like and PD-1+ CXCR5− Tim-3+ exhausted CD8 T cells from chronically infected mice were all sorted on day 45 postinfection. Naïve CD44^{lo}CD8 T cells were isolated from uninfected mice. All animal experiments were performed in accordance with Emory University Institutional Animal Care and Use Committee.

Fifty thousand sorted T cells were used for ATAC-seq analysis. Transcription factor binding site prediction analysis was performed using HOMER (42) and the chromVAR (43) package in R (44). Ingenuity pathway analysis was used to identify networks of genes with differential accessibility. Differentially accessible sites were assigned to genes based on regulatory domain associations as defined by GREAT (45).

ACKNOWLEDGMENTS. This work was supported by National Institutes of Health U19 AI057266 (to J.J.G.) and R01 AI030048 (to R.A.). P.L., J.-X.L., and W.J.L. are supported by the Division of Intramural Research, National Heart, Lung, and Blood Institute, NIH.

1. E. J. Wherry, T cell exhaustion. *Nat. Immunol.* **12**, 492–499 (2011).
2. A. J. Zajac *et al*., Viral immune evasion due to persistence of activated T cells without effector function. *J. Exp. Med.* **188**, 2205–2213 (1998).
3. A. Gallimore *et al*., Induction and exhaustion of lymphocytic choriomeningitis virus-specific cytotoxic T lymphocytes visualized using soluble tetrameric major histocompatibility complex class I-peptide complexes. *J. Exp. Med.* **187**, 1383–1393 (1998).
4. T. U. Vogel, T. M. Allen, J. D. Altman, D. I. Watkins, Functional impairment of simian immunodeficiency virus-specific CD8+ T cells during the chronic phase of infection. *J. Virol.* **75**, 2458–2461 (2001).
5. M. Dagarag, H. Ng, R. Lubong, R. B. Effros, O. O. Yang, Differential impairment of lytic and cytokine functions in senescent human immunodeficiency virus type 1-specific cytotoxic T lymphocytes. *J. Virol.* **77**, 3077–3083 (2003).
6. M. Hashimoto *et al*., CD8 T cell exhaustion in chronic infection and cancer: Opportunities for interventions. *Annu. Rev. Med.* **69**, 301–318 (2018).
7. K. E. Pauken, E. J. Wherry, Overcoming T cell exhaustion in infection and cancer. *Trends Immunol.* **36**, 265–276 (2015).
8. P. Sharma, J. P. Allison, The future of immune checkpoint therapy. *Science* **348**, 56–61 (2015).
9. D. L. Barber *et al*., Restoring function in exhausted CD8 T cells during chronic viral infection. *Nature* **439**, 682–687 (2006).
10. S. D. Blackburn *et al*., Coregulation of CD8+ T cell exhaustion by multiple inhibitory receptors during chronic viral infection. *Nat. Immunol.* **10**, 29–37 (2009).
11. V. Velu *et al*., Enhancing SIV-specific immunity in vivo by PD-1 blockade. *Nature* **458**, 206–210 (2009).
12. A. O. Kamphorst, R. Ahmed, Manipulating the PD-1 pathway to improve immunity. *Curr. Opin. Immunol.* **25**, 381–388 (2013).
13. K. M. Hargadon, C. E. Johnson, C. J. Williams, Immune checkpoint blockade therapy for cancer: An overview of FDA-approved immune checkpoint inhibitors. *Int. Immunopharmacol.* **62**, 29–39 (2018).
14. S. J. Im *et al*., Defining CD8+ T cells that provide the proliferative burst after PD-1 therapy. *Nature* **537**, 417–421 (2016).
15. R. He *et al*., Follicular CXCR5-expressing CD8(+) T cells curtail chronic viral infection. *Nature* **537**, 412–428 (2016).
16. D. T. Utzschneider *et al*., T cell factor 1-expressing memory-like CD8(+) T cells sustain the immune response to chronic viral infections. *Immunity* **45**, 415–427 (2016).
17. T. Wu *et al*., The TCF1-Bcl6 axis counteracts type I interferon to repress exhaustion and maintain T cell stemness. *Sci. Immunol.* **1**, eaai8593 (2016).
18. Y. A. Leong *et al*., CXCR5(+) follicular cytotoxic T cells control viral infection in B cell follicles. *Nat. Immunol.* **17**, 1187–1196 (2016).
19. B. Miles *et al*., Follicular regulatory CD8 T cells impair the germinal center response in SIV and ex vivo HIV infection. *PLoS Pathog.* **12**, e1005924 (2016).
20. G. H. Mylvaganam *et al*., Dynamics of SIV-specific CXCR5+ CD8 T cells during chronic SIV infection. *Proc. Natl. Acad. Sci. U.S.A.* **114**, 1976–1981 (2017).
21. C. Petrovas *et al*., Follicular CD8 T cells accumulate in HIV infection and can kill infected cells in vitro via bispecific antibodies. *Sci. Transl. Med.* **9**, eaag2285 (2017).
22. M. Sade-Feldman *et al*., Defining T cell states associated with response to checkpoint immunotherapy in melanoma. *Cell* **175**, 998–1013.e20 (2018).
23. I. Siddiqui *et al*., Intratumoral Tcf1(+)PD-1(+)CD8(+) T cells with stem-like properties promote tumor control in response to vaccination and checkpoint blockade immunotherapy. *Immunity* **50**, 195–211.e10 (2019).
24. B. C. Miller *et al*., Subsets of exhausted CD8$^+$ T cells differentially mediate tumor control and respond to checkpoint blockade. *Nat. Immunol.* **20**, 326–336 (2019).
25. A. N. Henning, R. Roychoudhuri, N. P. Restifo, Epigenetic control of CD8$^+$ T cell differentiation. *Nat. Rev. Immunol.* **18**, 340–356 (2018).
26. J. D. Buenrostro, P. G. Giresi, L. C. Zaba, H. Y. Chang, W. J. Greenleaf, Transposition of native chromatin for fast and sensitive epigenomic profiling of open chromatin, DNA-binding proteins and nucleosome position. *Nat. Methods* **10**, 1213–1218 (2013).
27. M. I. Love, W. Huber, S. Anders, Moderated estimation of fold change and dispersion for RNA-seq data with DESeq2. *Genome Biol.* **15**, 550 (2014).
28. A. O. Kamphorst *et al*., Rescue of exhausted CD8 T cells by PD-1-targeted therapies is CD28-dependent. *Science* **355**, 1423–1427 (2017).
29. S. M. Kaech, W. Cui, Transcriptional control of effector and memory CD8+ T cell differentiation. *Nat. Rev. Immunol.* **12**, 749–761 (2012).
30. A. Jalali *et al*., HeyL promotes neuronal differentiation of neural progenitor cells. *J. Neurosci. Res.* **89**, 299–309 (2011).
31. T. L. Stephen *et al*., SATB1 expression governs epigenetic repression of PD-1 in tumor-reactive T cells. *Immunity* **46**, 51–64 (2017).
32. S. Yao *et al*., Interferon regulatory factor 4 sustains CD8(+) T cell expansion and effector differentiation. *Immunity* **39**, 833–845 (2013).
33. P. Tripathi *et al*., STAT5 is critical to maintain effector CD8+ T cell responses. *J. Immunol.* **185**, 2116–2124 (2010).
34. G. Hu, J. Chen, A genome-wide regulatory network identifies key transcription factors for memory CD8$^+$ T-cell development. *Nat. Commun.* **4**, 2830 (2013).
35. A. E. Moran *et al*., T cell receptor signal strength in Treg and iNKT cell development demonstrated by a novel fluorescent reporter mouse. *J. Exp. Med.* **208**, 1279–1289 (2011).
36. L. L. Lau, B. D. Jamieson, T. Somasundaram, R. Ahmed, Cytotoxic T-cell memory without antigen. *Nature* **369**, 648–652 (1994).
37. S. M. Kaech *et al*., Selective expression of the interleukin 7 receptor identifies effector CD8 T cells that give rise to long-lived memory cells. *Nat. Immunol.* **4**, 1191–1198 (2003).
38. S. Sarkar *et al*., Functional and genomic profiling of effector CD8 T cell subsets with distinct memory fates. *J. Exp. Med.* **205**, 625–640 (2008).
39. N. S. Joshi *et al*., Inflammation directs memory precursor and short-lived effector CD8(+) T cell fates via the graded expression of T-bet transcription factor. *Immunity* **27**, 281–295 (2007).
40. B. Youngblood *et al*., Effector CD8 T cells dedifferentiate into long-lived memory cells. *Nature* **552**, 404–409 (2017).
41. R. S. Akondy *et al*., Origin and differentiation of human memory CD8 T cells after vaccination. *Nature* **552**, 362–367 (2017).
42. S. Heinz *et al*., Simple combinations of lineage-determining transcription factors prime cis-regulatory elements required for macrophage and B cell identities. *Mol. Cell* **38**, 576–589 (2010).
43. A. N. Schep, B. Wu, J. D. Buenrostro, W. J. Greenleaf, chromVAR: Inferring transcription-factor-associated accessibility from single-cell epigenomic data. *Nat. Methods* **14**, 975–978 (2017).
44. R Core Team, R: A Language and Environment for Statistical Computing (Version 3.5.2, R Foundation for Statistical Computing, Vienna, Austria, 2018). https://www.R-project.org/.
45. C. Y. McLean *et al*., GREAT improves functional interpretation of cis-regulatory regions. *Nat. Biotechnol.* **28**, 495–501 (2010).

Downloaded at Stanford University on November 16, 2021